

Microstructure and phase control in Bi–Fe–O multiferroic nanocomposite thin films

M. Murakami, S. Fujino, S.-H. Lim, L. G. Salamanca-Riba, M. Wuttig, and I. Takeuchi^{a)}
Department of Materials Science and Engineering, University of Maryland, College Park, Maryland 20742

Bindhu Varughese
Department of Chemistry, University of Maryland, College Park, Maryland 20742

H. Sugaya
Frontier Collaborative Research Center, Tokyo Institute of Technology, Yokohama 226-8503, Japan

T. Hasegawa
Department of Chemistry, Graduate School of Science, The University of Tokyo, 7-3-1 Hongo, Bunkyo-ku, Tokyo 113-0033, Japan

S. E. Lofland
Department of Physics and Astronomy, Rowan University, Glassboro, New Jersey 08028

(Received 22 September 2005; accepted 16 February 2006; published online 15 March 2006)

We report on the controlled multiphase thin film growth in the Bi–Fe–O system. By varying the deposition oxygen pressure, the dominant phase formed in the film continuously changes from ferroelectric BiFeO₃ to a mixture of α -Fe₂O₃ and ferromagnetic γ -Fe₂O₃. X-ray diffraction and high-resolution transmission electron microscopy have revealed that epitaxial multiferroic nanocomposites consisting of BiFeO₃ and Fe₂O₃ are formed when the deposition pressure is ≈ 5 mTorr. In order to investigate the previously reported anomalous enhancement in magnetization in BiFeO₃, we have fabricated a thickness gradient pure BiFeO₃ film. The out-of-plane lattice constant was found to increase continuously as the thickness is decreased from 300 to 5 nm, but no significant enhancement in magnetization was observed. © 2006 American Institute of Physics. [DOI: 10.1063/1.2184892]

Recently, BiFeO₃ has attracted much attention.^{1,2} There have been a number of reports on thin film BiFeO₃, but their multiferroic properties have not been unambiguously established.^{3,4} Recently, Béa *et al.* have reported on the parasitic phases in BiFeO₃ thin films.⁵ However, detailed study of the microstructure of the films was not presented. In this study, we report on the microstructural properties of multiphase bismuth iron oxide thin films using transmission electron microscopy (TEM). Coexisting BiFeO₃ and Fe₂O₃ phases (α and γ) are observed in the films with a systematically varying degree of mixture controlled by the deposition oxygen partial pressure. The columnar epitaxial mixture of ferroelectric BiFeO₃ and Fe₂O₃ represents a new type of multiferroic nanocomposite material.

In order to fabricate bismuth iron oxide thin films by pulsed laser deposition, we ablated a stoichiometric BiFeO₃ target with a KrF excimer laser ($\lambda=248$ nm) with a typical fluence of 2 J/cm². The oxygen pressure and the substrate temperature during the deposition were varied in the ranges of 0.025–100 mTorr and 550–750 °C, respectively. The typical deposition rate was 5 nm/min, and SrTiO₃ (STO) (001) was used as the substrate. Scanning x-ray microdiffraction (using a D8 DISCOVER with GADDS for combinatorial screening by Bruker-AXS) and TEM were used for structural characterization of the films. TEM images and selected area diffraction (SAD) patterns of the films were obtained at an accelerating voltage of 300 keV using a JEOL 4000-FX

TEM. A superconducting quantum interference device (SQUID) magnetometer and a low temperature scanning SQUID microscope were used to perform magnetic characterization.

Figure 1 shows x-ray diffraction (XRD) spectra of the 300 nm thick bismuth iron oxide thin films deposited under different oxygen pressures. Diffraction was performed using the ω -scan mode, and the intensities were integrated in χ between 85° and 95°. Epitaxial BiFeO₃ films with the [001] axis perpendicular to the substrate surface were obtained at oxygen pressure higher than 1 mTorr, and the intensity of the (002) diffraction peaks of the BiFeO₃ increases as the

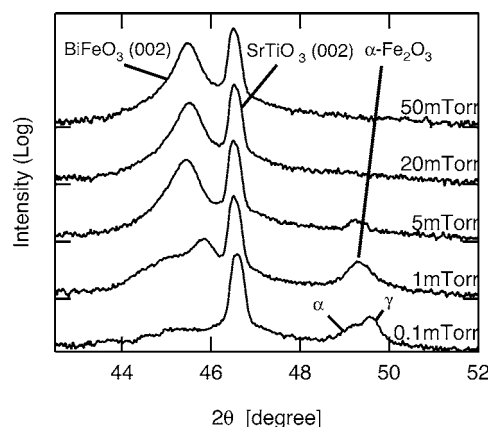


FIG. 1. (Color online) X-ray diffraction (in log scale) of bismuth iron oxide thin films deposited under different oxygen partial pressures.

^{a)}Also at: Center for Superconductivity Research, University of Maryland, College Park, MD 20742; electronic mail: takeuchi@umd.edu

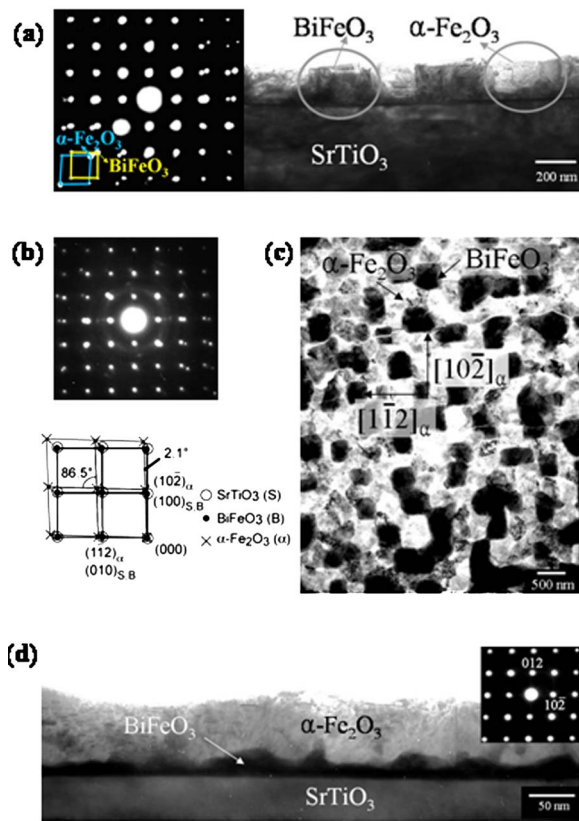


FIG. 2. (Color online) TEM bright field images and SAD patterns of bismuth iron oxide thin films fabricated on (001) SrTiO_3 substrates: (a) cross-sectional image and SAD pattern of the film deposited at 1 mTorr; (b) plan view SAD pattern with schematic; (c) plan view image of the same film as (b) deposited at 1 mTorr; and (d) cross-sectional image and corresponding SAD pattern of a film deposited at 0.1 mTorr.

pressure increases. Bi_2O_3 phase was also observed at oxygen pressure higher than 50 mTorr.⁵ We also observe peaks corresponding to the $\alpha\text{-Fe}_2\text{O}_3$ phase with the $[012]$ orientation when the oxygen pressure is less than 5 mTorr, and the intensity of these peaks increases as the oxygen pressure decreases. A mixture of BiFeO_3 and $\alpha\text{-Fe}_2\text{O}_3$ phases was observed for the deposition pressure between 1 and 5 mTorr. This transition in the dominant phase in the film reflects the change in the amount of the Bi incorporation in the films due to the high volatility of Bi metal. As we decrease the deposition oxygen pressure, the Bi content in the films decreases. When the deposition pressure is less than 1 mTorr, we also see a peak from $\gamma\text{-Fe}_2\text{O}_3$. At the oxygen pressure of 20 mTorr, the film is single phase BiFeO_3 , and it shows a monoclinically distorted (by about 0.5°) tetragonal structure. The lattice constants of the BiFeO_3 calculated from electron diffraction data (not shown) are $a=0.394$ nm, $c=0.398$ nm. The films are relaxed at a thickness of 300 nm, and these lattice parameters agree with ones reported by others.^{2,6} We do not observe any impurity phases in films deposited under this condition. We believe the shift in the (002) diffraction at 1 mTorr is caused by relaxation of BiFeO_3 resulting from stabilization of the phase separated configuration of BiFeO_3 and Fe_2O_3 phases. The smaller broad (002) peak corresponding to a larger lattice constant is likely from the thin layer of strained BiFeO_3 at the substrate interface discussed below.

Figure 2 shows TEM images of 200 nm thick bismuth iron oxide thin films. BiFeO_3 and Fe_2O_3 phases were found to have grown epitaxially with respect to the substrate as

well as with respect to each other in the lateral direction in a columnar manner. We have found that the Fe_2O_3 domains grow with a mixture of α and γ phases, with α being the predominant phase. Fig. 2(a) is a cross-sectional bright field image of the film showing the presence of BiFeO_3 and $\alpha\text{-Fe}_2\text{O}_3$. This film was grown at 1 mTorr of oxygen. The corresponding SAD pattern from the $\alpha\text{-Fe}_2\text{O}_3$ was identified as the superposition of the (100) pattern from BiFeO_3 and that of the rhombohedral crystal structure of $\alpha\text{-Fe}_2\text{O}_3$ (space group: $R\bar{3}c$) with lattice constants of $a=b=0.505$ nm, $c=1.319$ nm, which are in good agreement with the published structure (i.e., JCPDS No. 33-0664). We have also confirmed this result with energy dispersive x-ray spectroscopy. The epitaxial relationship of BiFeO_3 and $\alpha\text{-Fe}_2\text{O}_3$ was determined from the electron diffraction patterns of the cross-sectional view [inset of Fig. 2(a)] and the plan view [Fig. 2(b)]: $[001]_{\text{BiFeO}_3}$ is seen to be almost parallel (within 0.2°) to $[001]_{\text{STO}}$ (corresponding to the out-of-plane direction). However, $[012]$ of $\alpha\text{-Fe}_2\text{O}_3$ is deviated by 2.1° from $[001]_{\text{BiFeO}_3}$. Figure 2(c) is a plan view TEM image taken from the same sample grown at 1 mTorr. The interface between BiFeO_3 and $\alpha\text{-Fe}_2\text{O}_3$ is parallel to the $[10\bar{2}]$ and $[1\bar{1}\bar{2}]$ directions of $\alpha\text{-Fe}_2\text{O}_3$. From the electron diffraction patterns, $[100]_{\text{BiFeO}_3}$ is seen to be almost parallel to $[100]_{\text{STO}}$ (corresponding to the in-plane direction), with the in-plane lattice parameters of 0.394 and 0.3905 nm, respectively. However, $[10\bar{2}]$ of $\alpha\text{-Fe}_2\text{O}_3$ makes an angle of $\sim 2.1^\circ$ with respect to the $[100]_{\text{BiFeO}_3}$. The measured interplanar distance between (000) and $(10\bar{2})$ of $\alpha\text{-Fe}_2\text{O}_3$ is 0.370 nm, which is slightly larger than a published result (0.3684 nm, JCPDS No. 33-0664) for bulk $\alpha\text{-Fe}_2\text{O}_3$. These results can be explained as a consequence of an in-plane tensile stress imposed by BiFeO_3 on the $\alpha\text{-Fe}_2\text{O}_3$. The increase of the $(10\bar{2})$ interplanar distance gives rise to a decrease in the (012) interplanar distance, which was measured as 0.364 nm. The lattice mismatch strain between BiFeO_3 and $\alpha\text{-Fe}_2\text{O}_3$ is 7.1%. After relaxation, a residual strain of 5.9% was calculated from our TEM and XRD results. Fig. 2(d) shows a bismuth iron oxide thin film fabricated at 0.1 mTorr. At this low pressure, the dominant phase is $\alpha\text{-Fe}_2\text{O}_3$ which forms a continuous layer on a thin layer (≈ 5 nm) of BiFeO_3 above the substrate. The fact that $\alpha\text{-Fe}_2\text{O}_3$ appears to have grown above BiFeO_3 indicates that it nucleated at the top surface of the film as Bi atoms vaporized following deposition. In a recent letter,⁵ a mixture of BiFeO_3 and $\gamma\text{-Fe}_2\text{O}_3$ (maghemite) grown at low oxygen partial pressure was reported. Their XRD results and magnetic properties are consistent with the second phase being $\gamma\text{-Fe}_2\text{O}_3$. However, in our experiments, the dominant phase at low oxygen partial pressure was revealed to be $\alpha\text{-Fe}_2\text{O}_3$ from the TEM analysis. The SAD pattern in the inset of Fig. 2(d) taken from the iron oxide area was indexed to $\alpha\text{-Fe}_2\text{O}_3$ and the measured angle ($\sim 86.5^\circ$) between (012) and $(10\bar{2})$ agrees well with the calculated angle (86.0°) in rhombohedral bulk $\alpha\text{-Fe}_2\text{O}_3$. However, we also found a small trace of γ phase precipitates with a plate-like shape embedded in the α -phase matrix. Indeed, in XRD in Fig. 1, a peak from $\gamma\text{-Fe}_2\text{O}_3$ is located fairly close to that of $\alpha\text{-Fe}_2\text{O}_3$. We have not studied the influence of temperature on the nanostructure of the films in detail, but we expect similar trends in structure changes when either the oxygen partial pressure is decreased or the deposition temperature is in-

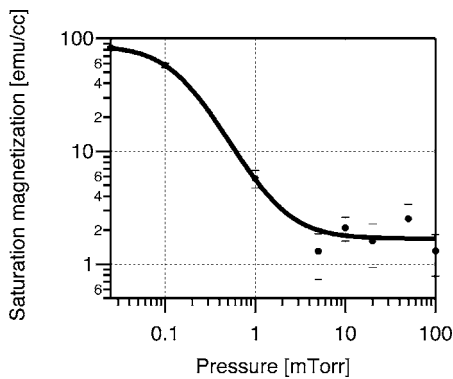


FIG. 3. (Color online) Room temperature saturation magnetization (emu/cc) of Bi-Fe-O films as a function of oxygen pressure during the deposition.

creased. Details of the microstructural properties of the BiFeO₃-Fe₂O₃ mixture will be reported elsewhere.

Figure 3 shows the saturation magnetization of the various BiFeO₃-Fe₂O₃ films (≈ 300 nm thick) measured by a SQUID magnetometer at room temperature. The magnetization of the bismuth iron oxide films fabricated at oxygen partial pressures higher than 5 mTorr is about 2 emu/cc. This value is consistent with that of pure BiFeO₃ thin films previously reported by others.^{3,5,7} The magnetization of the films increases steadily as the deposition pressure decreases, and reaches about 80 emu/cc, for the film fabricated at 0.1 mTorr. α -Fe₂O₃ (hematite) is known to exhibit weak ferromagnetism below the Néel temperature ($T_N \approx 950$ K).^{8,9} In contrast, γ -Fe₂O₃ is known to display magnetization up to 400 emu/cc at room temperature.¹⁰ Assuming that the magnetization observed here arises from γ -Fe₂O₃, we estimate the volume fraction of γ -Fe₂O₃ to be $\leq 20\%$ in the films deposited at less than 1 mTorr. This is consistent with x-ray results shown in Fig. 1, which shows that the γ -Fe₂O₃ peak is only “visible” in the spectra from films deposited at the lowest pressure. This shows that we can controllably tune the magnetization of the Bi-Fe-O films by adjusting the deposition pressure in the 0.1–5 mTorr range, which in turn determines the multiphase mixture ratio.

Our BiFeO₃ films have exhibited good piezoelectric properties at room temperature as measured by piezoelectric force microscopy.¹¹ Magnetostriction in α -Fe₂O₃ as well as γ -Fe₂O₃ has been previously reported.^{12,13} The present films, which are epitaxial nanocomposite mixtures of magnetostrictive α -Fe₂O₃ and piezoelectric BiFeO₃, thus represent a new type of composite multiferroic material. Investigation of the ME coupling in the BiFeO₃-Fe₂O₃ composite films is currently underway.¹⁴

Stress enhanced magnetization in excess of 100 emu/cc was previously observed in BiFeO₃ films.² Eerenstein *et al.* have also studied thickness dependent magnetization in BiFeO₃ films, but observed no enhancement.³ To further systematically study the stress enhancement effect in thin films, we grew a BiFeO₃ film sample with a continuously changing thickness by a gradient deposition technique using a moving shadow mask.¹⁵ Figure 4 shows the out-of-plane lattice constant and the intensity of the BiFeO₃ (002) peak measured by

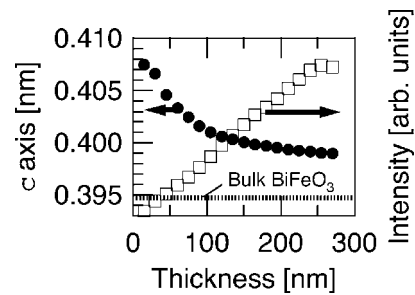


FIG. 4. (Color online) Lattice constant (left) and intensity (right) of (002) BiFeO₃ peak observed by microdiffraction as a function of continuously changing film thickness.

x-ray microdiffraction. The lattice constant decreases, and the peak intensity increases continuously as the thickness increases. This plot indicates that the stress in the film decreases as the thickness increases and the degree of relaxation increases continuously. We have performed scanning SQUID microscopy across this sample and found that the magnetization of the film does not change. X-ray photoelectron spectroscopy of this sample revealed that the valence state of Fe in the film remains 3+ in the thickness range studied here. These results are consistent with those reported by Eerenstein *et al.*³

The authors acknowledge V. Nagarajan and A. Varatharajan for piezoelectric force microscopy measurement and useful discussions. This work was supported by Grant Nos. ONR N000140110761, ONR N000140410085, NSF DMR 0094265 (CAREER), NSF DMR 0231291, MRSEC DMR 0520471 and NSF 0095166.

¹G. A. Smolenskii and I. Chupis, *Sov. Phys. Usp.* **25**, 475 (1982).

²J. Wang, J. B. Neaton, H. Zheng, V. Nagarajan, S. B. Ogale, B. Liu, D. Viehland, V. Vaithyanathan, D. G. Schlom, U. V. Waghmare, N. A. Spaldin, K. M. Rabe, M. Wuttig, and R. Ramesh, *Science* **299**, 1719 (2003).

³W. Eerenstein, F. D. Morrison, J. Dho, M. G. Blamire, J. F. Scott, and N. D. Mathur, *Science* **307**, 1203a (2005).

⁴J. Wang, A. Scholl, H. Zheng, S. B. Ogale, D. Viehland, D. G. Schlom, N. A. Spaldin, K. M. Rabe, M. Wuttig, L. Mohaddes, J. Neaton, U. Waghmare, T. Zhao, and R. Ramesh, *Science* **307**, 1203b (2005).

⁵H. Béa, M. Bibes, A. Barthélémy, K. Bouzouane, E. Jacquet, A. Khodan, J.-P. Contour, S. Wycisk, A. Forget, D. Lebeugle, D. Colson, and M. Viret, *Appl. Phys. Lett.* **87**, 072508 (2005).

⁶X. Qi, M. Wei, Y. Lin, Q. Jia, D. Zhi, J. Dho, M. G. Blamire, and J. L. MacManus-Driscoll, *Appl. Phys. Lett.* **86**, 071913 (2005).

⁷K. Y. Yun, M. Noda, M. Okuyama, H. Seki, H. Tabata, and K. Saito, *J. Appl. Phys.* **96**, 3399 (2004).

⁸Y.-Y. Li, *Phys. Rev.* **101**, 1450 (1956).

⁹R. Z. Levitin, A. S. Pakhomov, and V. A. Shchurov, *Sov. Phys. JETP* **29**, 669 (1969).

¹⁰A. J. Koch, J. J. Becker, A. E. Berkowitz, W. J. Schuele, and P. J. Flanders, *J. Appl. Phys.* **39**, 1261 (1968).

¹¹V. Nagarajan, S. Aggarwal, A. Gruverman, R. Ramesh, and R. Waser, *Appl. Phys. Lett.* **86**, 262910 (2005).

¹²R. A. Voskanyan, R. Z. Levitin, and V. A. Shchurov, *Sov. Phys. JETP* **27**, 423 (1968).

¹³M. Langlet and J. C. Joubert, *IEEE Trans. Magn.* **24**, 1691 (1988).

¹⁴C. Gao, B. Hu, X. Li, C. Liu, M. Murakami, K.-S. Chang, C. J. Long, M. Wuttig, and I. Takeuchi, *Appl. Phys. Lett.* **87**, 153505 (2005).

¹⁵R. Takahashi, H. Kubota, M. Murakami, Y. Yamamoto, Y. Matsumoto, and H. Koinuma, *J. Comb. Chem.* **6**, 50 (2004).